



## QUANTUM FISHER INFORMATION AND QUANTUM DISCORD IN THE TWO-QUBIT SPIN CHAIN WITH DZIALOSHINSKII- MORIYA INTERACTION

 Nour Zidan<sup>1\*</sup>,  Ahmed Redwan<sup>2</sup>, Hamada Adel-Hameed<sup>3,4</sup>,  
Tarek El-Shahat<sup>2</sup>

<sup>1</sup>Mathematics Department, College of Science, Jouf University, Sakaka, Saudi Arabia

<sup>2</sup>Mathematics Department, Faculty of Science, Al-Azhar University, 71524 Assiut, Egypt

<sup>3</sup>Mathematics Department, Faculty of Science, Sohag University, Sohag, Egypt

<sup>4</sup>Mathematics Department, Khurma University College, Taif University, Al-Taif, Saudi Arabia

---

**Abstract.** We investigate the performance of Quantum Fisher Information (QFI) and Quantum Discord (QD) in a two-qubit spin system with Dzyaloshinskii-Moriya (DM) interaction in the presence of an external magnetic field. The current dynamical maps of QFI and QD are investigated by characterizing these functions of the DM interaction, magnetic field strength, and temperature. Parameter optimization can achieve maximal and prolonged QFI and QD under DM interaction in a two-qubit spin chain. The QFI and QD decay monotonically, with no signs of revival, implying they are permanently lost. Although the effects of magnetic field and temperature are both degrading, we find that their consequences can be controlled by increasing the number of DM interactions available, resulting in longer QD and QFI preservation.

---

**Keywords:** Thermal Entanglement, Quantum Fisher Information, Quantum Discord, Dzyaloshinskii-Moriya interaction.

**AMS Subject Classification:** 81P15, 81P43.

**Corresponding author:** Nour Zidan, Mathematics Department, College of Science, Jouf University, Sakaka, Saudi Arabia, e-mail: [nazidane@ju.edu.sa](mailto:nazidane@ju.edu.sa)

*Received:* 9 September 2023; *Revised:* 30 October 2023; *Accepted:* 27 November 2023;

*Published:* 20 December 2023.

---

## 1 Introduction

Fisher's information is helpful in engineering statistics Korashy et al. (2021) Ganaie et al. (2021) and the representation of variable quantum equations of motion Chentsov (1982) Abdel-Khalek et al. (2017). It was first developed for statistical modeling, and the Cramér-Rao inequality limits the accuracy of estimation based on Fisher information. This information has the most miniature precision (variance) of all quantifications. There is also a quantum version of the Cramer-Rao inequality, and Fisher's information has also been applied to quantum scenarios Oleiwi et al. (2023) Xu & Chen (2018). In addition, several fractional models have been investigated El-Sayed et al. (2023) Sweilam & Abou Hasan (2016).

When we need to assess the model parameters, we can identify neighboring distributions along the parametric curve Cremér (1946) Fakharany (2022). A generalized family of probability densities, denoted as  $P(x)$  where  $x$  is variable and is the parameter, can help us evaluate this

---

**How to cite (APA):** Zidan, N., Redwan, A., Adel-Hameed, H., & El-Shahat, T. (2023). Quantum Fisher Information and quantum discord in the two-qubit spin chain with Dzyaloshinskii-Moriya interaction. *Advanced Mathematical Models & Applications*, 8(3), 452-463.

parameter value by differentiating between adjacent distribution functions along the parametric curve. With extensive Fisher Information, we can make more confident predictions about the parameter. In a quantum situation, we can use the quantum Cramér–Rao bound to determine the expansion of Fisher Information Braunstein (1996) El-Sanousy (2021) . Since its inception, QFI has undergone thorough research from various perspectives. Discussions have focused on improving precision estimation Boixo et al. (2007), measuring optimization Ma et al. (2011) and exploring QFI’s characteristics and applicability Luo (2004).

Parameter estimation and quantum phase transitions have gained attention Sun et al. (2010) Salvatori et al. (2014). Advancements in Quantum Fisher Information have led to better characterization of system-cavity couplings, creating quantum systems with higher entanglement.

Extensive research has been conducted on Quantum Fisher Information (QFI) in various fields, such as characterizing quantum phase transitions Invernizzi et al. (2008), exploring uncertainty relations Luo (2000) Gibilisco et al. (2007), estimating quantum speedup limits, and detecting entanglement Boixo & Monras (2008). Notably, studies have been conducted on the influence of Unruh in the non-inertial framework on quantification Metwally (2018) Banerjee et al. (2016). QFI has also been studied for multi-particle entangled states, including spin chains Ozaydin, & Altintas (2020) Alenezi et al. (2022) the Lipkin-Meshkov-Glick model Ma & Wang (2009), atom-cavity systems Zidan et al. (2019), and superconducting charge qubits Abdel-Hameed et al. (2018). Exciting research has been done in these areas, including studies on entangled states such as Apellaniz et al. (2015).

Additionally, an interesting study examined the thermal quantum discord in various Heisenberg models, as referenced in sources Zhu & Zhang (2012) Redwan, & El-Shahat (2017). The research found that thermal quantum entanglement is stronger than thermal entanglement with temperature. This study also found that quantum discord (QD) remains present at lower temperatures, while thermal entanglement disappears entirely at a specific temperature. Therefore, QD is a more realistic way to express quantum correlation than entanglement. Recent extensive research has focused on entanglement and quantum correlation in a diatomic system interacting with a single-mode cavity field, including Fock state, thermal field state, coherent field state, and more, as cited in sources Zidan (2014) Bakry et al. (2018).

Spin-orbit coupling impacts non-classical correlations in quantum mechanics and information. Zhang’s research showed that Dzyaloshinskii-Moriya (DM) interaction can cause thermal entanglement in ferromagnetic and anti-ferromagnetic Heisenberg models. The ferromagnetic model is better for quantum teleportation with DM interaction. Two and three-level systems with magnetic fields were studied, showing DM interaction overcomes decoherence effects on entanglement from thermalization and external fields Dzyaloshinskii (1958) Song et al. (2014).

In this work, we will be delving into a detailed examination of the QFI and QD of a two-qubit spin system that displays DM interaction, while also being subjected to an external magnetic field. Our study will include an investigation into the effect of temperature and magnetic field on the system’s thermal entanglement. The results are quite intriguing, as we discovered that the DM interaction has a profound impact on the thermal entanglement of the system. Additionally, we found that selecting the appropriate strength of DM interaction at higher temperatures can lead to further improvement of the thermal entanglement. The structure of the paper is summarized below. In section 2, we explain the two-bit spin system and calculate its density matrix. We compare numerical modeling results to other model parameters in sections 3 and 4, such as (QFI) and (QD). Finally, we describe our findings in the 5 section.

## 2 Model and solution for a two-qubit

The Hamiltonian for a two-qubit anisotropic Heisenberg model with z-component interaction parameter  $D_z$  is

$$\begin{aligned} H &= J(1 + \gamma)\sigma_1^x\sigma_2^x + J(1 - \gamma)\sigma_1^y\sigma_2^y \\ &+ D_z(\sigma_1^x\sigma_2^y - \sigma_1^y\sigma_2^x) + B(\sigma_1^z + \sigma_2^z), \end{aligned} \quad (1)$$

where  $J$  is the real coupling coefficient,  $\gamma$  is the anisotropic parameter,  $D_z$  is the z-component DM interaction parameter,  $B$  the external magnetic field, and  $\sigma^i (i = x, y, z)$  are Pauli matrices.

The eigenvalues the Hamiltonian  $H$  are given by

$$\begin{aligned} E_1, E_2 &= \pm 2\alpha, \quad \alpha = \sqrt{B^2 + J^2\gamma^2}, \\ E_3, E_4 &= \pm 2\beta, \quad \beta = \sqrt{D_z^2 + J^2} \end{aligned} \quad (2)$$

with crossposting eigenvectors given by

$$\begin{aligned} |E_1\rangle &= \frac{1}{\sqrt{2\alpha(\alpha - B)}}(-(\alpha - B)|00\rangle + J\gamma|11\rangle) \\ |E_2\rangle &= \frac{1}{\sqrt{2\alpha(\alpha - B)}}((\alpha + B)|00\rangle + J\gamma|11\rangle) \\ |E_3\rangle &= \frac{1}{\sqrt{2}}(e^{i\theta}|10\rangle + |01\rangle) \\ |E_4\rangle &= \frac{1}{\sqrt{2}}(-e^{i\theta}|10\rangle + |01\rangle) \end{aligned} \quad (3)$$

where  $\theta = \tan^{-1}(\frac{D_z}{J})$

At thermal equilibrium of temperature  $T$ , in the standard basis  $\{|00\rangle, |01\rangle, |10\rangle, |11\rangle\}$  the density operator for the system under consideration can be worked out to be

$$\rho(T) = \frac{1}{Z} \exp \left[ -\frac{H}{\kappa_\beta T} \right], \quad (4)$$

where  $z$  is the partition function of the system and  $\kappa_\beta$  is the Boltzmann constant (for simplicity we put  $\kappa_\beta = 1$ ). Based on the eigenvectors  $|E_i\rangle (i = 1, 2, 3, 4)$  and the eigenvalues  $E_i$  of the Hamiltonian Eq. (1), the explicit form of the thermal matrix  $\rho(T)$  can be expressed as the density matrix of the system in the thermal equilibrium can be obtained as

$$\rho(T) = \begin{pmatrix} \rho_{11} & 0 & 0 & \rho_{14} \\ 0 & \rho_{22} & \rho_{23} & 0 \\ 0 & \rho_{32} & \rho_{33} & 0 \\ \rho_{41} & 0 & 0 & \rho_{44} \end{pmatrix}, \quad (5)$$

where

$$\begin{aligned} \rho_{11} &= \frac{1}{Z\alpha} \left[ \alpha \cosh \left( \frac{2\alpha}{T} \right) - B \sinh \left( \frac{2\alpha}{T} \right) \right], \\ \rho_{44} &= \frac{1}{Z\alpha} \left[ \alpha \cosh \left( \frac{2\alpha}{T} \right) + B \sinh \left( \frac{2\alpha}{T} \right) \right], \\ \rho_{14} &= \rho_{41} = -\frac{J\gamma}{Z\alpha} \sinh \left( \frac{2\alpha}{T} \right), \\ \rho_{22} &= \rho_{33} = \frac{1}{Z} \cosh \left( \frac{2\beta}{T} \right), \\ \rho_{23} &= \rho_{32}^* = \frac{1}{Z} e^{-i\theta} \sinh \left( \frac{2\beta}{T} \right), \\ Z &= 2 \left[ \cosh \left( \frac{2\beta}{T} \right) + \cosh \left( \frac{2\alpha}{T} \right) \right]. \end{aligned} \quad (6)$$

### 3 Quantum Fisher Information

We briefly review the main aspects of the QFI. In classical statistical inference theory, Fisher information is used to measure the amount of information about an unknown parameter  $\theta$  from the measurement results of an observable variable  $X$ . The classical Fisher information with respect to the parameter  $\theta$  is defined as Fisher (1925)

$$G(\theta) = \sum_i P_i(x|\theta) \left[ \frac{\partial}{\partial \theta} \ln P_i(x|\theta) \right]^2 \quad (7)$$

where  $P_i(x|\theta)$  denotes the probability density of the measurement outcome  $x_i$  conditioned on the fixed parameter  $\theta$ . By diagonalizing the density matrix

$$\rho(\theta) = \sum_{i=1}^M \lambda_i(\theta) |\psi_i(\theta)\rangle \langle \psi_i(\theta)| \quad (8)$$

Here  $\lambda_i(\theta), |\psi_i(\theta)\rangle$  are the  $i$ th eigenvalue and eigenstate of the density matrix, respectively.  $M$  is the rank of the density matrix  $\rho(\theta)$ , the QFI for a non-full rank density matrix Jing et al. (2014)

$$\begin{aligned} F &= \sum_{i=1}^M \frac{(\partial_\theta \lambda_i)^2}{\lambda_i} + 4 \sum_{i=1}^M \lambda_i [\langle \partial_\theta \psi_i | \partial_\theta \psi_i \rangle - |\langle \psi_i | \partial_\theta \psi_i \rangle|^2] \\ &- 8 \sum_{i \neq k}^M \frac{\lambda_i \lambda_k}{\lambda_i + \lambda_k} |\langle \psi_i | \partial_\theta \psi_k \rangle|^2. \end{aligned} \quad (9)$$

Accurate identification of the eigenvalues and eigenvectors of the reduced density operator defined by Eq. (5) is crucial to determine the quantum Fisher information of the system. The eigenvalues are obtained as

$$\begin{aligned} \lambda_{1,2} &= \cosh(2\alpha/T) \mp \sinh(2\alpha/T) \\ \lambda_{3,4} &= \cosh(2\beta/T) \mp \sinh(2\beta/T), \end{aligned} \quad (10)$$

with corresponding eigenvectors are

$$\begin{aligned} |\psi_1\rangle &= (a_1, 0, 0, b_1), & |\psi_2\rangle &= (a_2, 0, 0, b_2), \\ |\psi_3\rangle &= \frac{1}{\sqrt{2}}(0, e^{-i\theta}, 1, 0), & |\psi_4\rangle &= \frac{1}{\sqrt{2}}(0, -e^{-i\theta}, 1, 0), \end{aligned} \quad (11)$$

where

$$\begin{aligned} a_1 &= \frac{-(\alpha + B)}{\sqrt{2\alpha(\alpha + B)}}, & b_1 &= \frac{J\gamma}{\sqrt{2\alpha(\alpha + B)}}, \\ a_2 &= \frac{\alpha - B}{\sqrt{2\alpha(\alpha - B)}}, & b_2 &= \frac{J\gamma}{\sqrt{2\alpha(\alpha - B)}}, \end{aligned} \quad (12)$$

#### 3.1 Quantum Fisher information with respect to magnetic field B

In this section, we use the quantum Fisher information to precisely determine the magnetic field parameter  $B$ . This method provides a more accurate and dependable estimate of the parameter, which is crucial for various scientific and technological applications. According to the definition



in Eq. (9) and using Eqs. (10) and (11), the exact formula of quantum Fisher information with respect to  $B$  (QFI) is obtained as

$$QFI = \frac{4}{T^2 Z^2 \alpha^4} \left( J^2 \gamma^2 T^2 \sinh^2 \left( \frac{2\alpha}{T} \right) \left[ 1 + \cosh \left( \frac{2\beta}{T} \right) \operatorname{sech} \left( \frac{2\alpha}{T} \right) \right] + 4B^2 \alpha^2 \left[ 1 + \cosh \left( \frac{2\beta}{T} \right) \cosh \left( \frac{2\alpha}{T} \right) \right] \right). \quad (13)$$

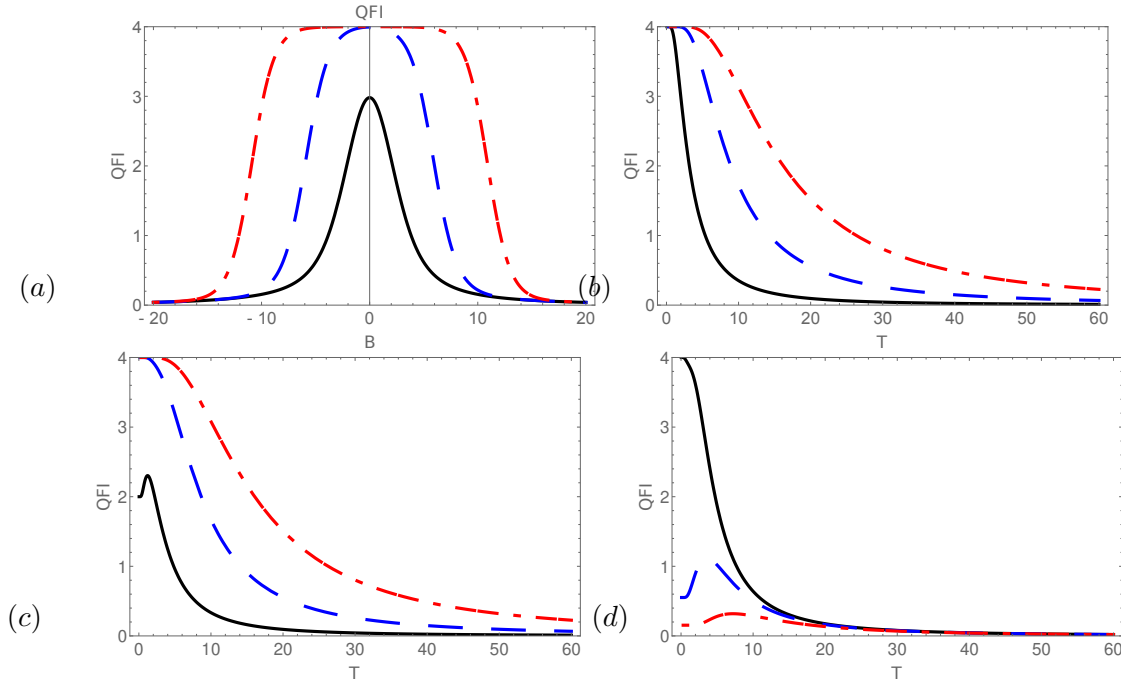


**Figure 1:** (a) The evolution of Quantum Fisher Information (QFI) in terms of  $B$ . The solid, dashed and dot-dashed curves are evaluated for  $D = 0, 5, 10$ , respectively, with  $T = 2$ . The QFI as a function of temperature  $T$ . The solid, dashed and dot-dashed curves are evaluated for  $D = 0, 5, 10$ , respectively where in (b)  $B = 0$ , (c)  $B = 2$  and in (d) the solid, dashed and dot-dashed curves are evaluated for  $B = 1, 5, 10$ , respectively, with  $D = 2$ . ( $\gamma = 2, J = 1$ )

Fig.1 addresses the dynamics of QFI in a two-qubit anisotropic Heisenberg model while considering different interactions such as DM, temperature, and magnetic effects and corresponding parameters. We witnessed that in these other interactions and plotting against various parameters, the dynamics of the two qubits seem increasingly different. The rise and fall maps of the QFI under different situations do not match each other. For example, in Fig.1(a), we plotted the QFI as a function of the external magnetic field. We noticed that for the increasing choices of magnetic field strength  $B$ , the width of the slopes becomes more comprehensive, and the QFI seems more preserved. Besides, QFI as a function of  $B$  also shows preservation enhancement for the high values of DM interacting strength  $D_z$ . The statement can be justified by comparing the graphs obtained for  $D_z = 0, 5$  and  $10$ , where the width of the preservation is greater at  $D_z = 10$ . Thus, both parameters can enhance quantum information preservation for longer intervals. It's also worth noting that when there's no magnetic field, the QFI rises to a maximum of 4 before rapidly falling. The QFI steadily decays as the DM interaction increases, as shown in Fig.1(b). Furthermore, as  $T$  increases, the QFI measure rapidly degrades and eventually achieves the lowest conceivable saturation level. As a result,  $T$  and QFI survival have an inverse relationship. The QFI starts at 2 and decays to  $D_z = 0$  when an external magnetic field is present, but the QFI obtains the highest initial encoded value when  $B = 2$ . As a result, as shown in Fig.1, the value of QFI with  $T$  is determined by the value of  $B$ , and it lowers as

$B$  grows (c). In addition, as the DM interaction  $D_z = 5, 10$  was increased, the QFI rose to a high of 4 before gradually decreasing, as seen in Fig.1(c). In 1(d), we studied the influence of a magnetic field on QFI at different levels of DM interaction. As we discovered, the QFI starts at value 4 at  $B = 1$  and rapidly decays. As  $B$  rises, the QFI drops, which is in line with Fig.1(c).

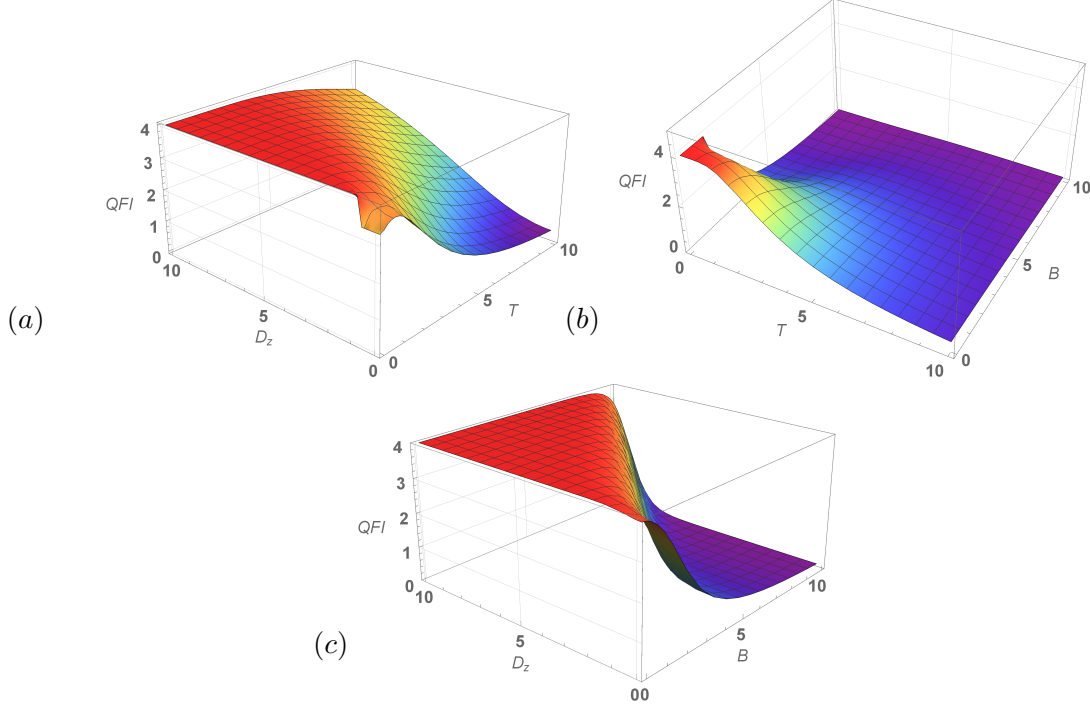


**Figure 2:** The evolution of Quantum Fisher Information (QFI) against the different parameters. In (a) be plotted between  $T$ ,  $D_z$  at  $B = 1$ , (b) be plotted between  $T$ ,  $B$  at  $D_z = 1$ , (c) be plotted between  $B$ ,  $D_z$  at  $T = 1$ . ( $\gamma = 2, J = 1$ )

Fig.2, we disclose the dynamics of QFI against different parameter ranges. In Fig.2(a), we plotted the dynamical map of QFI while considering the effects of  $D_z$  and  $T$  while keeping  $B$  constant at unity. We find that with increasing choices of  $D_z$ , the QFI becomes higher. At  $D_z = 10$ , we witnessed the QFI reaching the highest elevation. Thus, increasing the  $D_z$  means an enhancement in the QFI measure. Besides, against the increasing values of  $T$ , we find the QFI decaying monotonically. In case of Fig.2(b), we plotted the effects parameters  $T$  and  $B$ . Under both parameters' combined effects, QFI decays faster than that observed in Fig.2(a). In Fig.2(c), we plotted the effects of  $D_z$  and  $B$  over the QFI dynamical map. The current results are interesting, and both the parameters affected the QFI map oppositely. The  $D_z$  parameter enhances the QFI function, while the magnetic strength parameter reduces the QFI. The QFI function finally becomes zero at  $T > 5$  while maximum at  $D_z > 5$ .

## 4 Quantum Discord (QD)

Quantum discord (QD) is based on the distinction between quantum collaborative information and classical correlation. In a two-qubit quantum system, the overall correlation is measured using their quantum collaborative information, denoted by  $L(\rho_{ab}) = S(\rho_a) + S(\rho_b) - S(\rho_{ab})$ , where  $\rho_{a(b)}$  and  $\rho_{ab}$  represent the reduced density matrix of  $\rho_{a(b)}$  and the density of the binary system singly. Here,  $S(\rho) = -\text{tr}(\rho \log_2 \rho)$  is the von Neumann entropy. (QD) is a measurement of the quantumness of correlation between A and B and is also defined as the difference between total correlation and classical correlation. For the X state described by the density matrix, (QD) is given by:

$$QD = \min[D_1, D_2] \quad (14)$$

with

$$QD_j = \Gamma(\rho_{11} + \rho_{33}) + \sum_{k=1}^4 \lambda_k \log_2 \lambda_k + R_j$$

and

$$R_1 = -\Gamma(\rho_{11} + \rho_{33}) - \sum_{i=1}^4 \rho_{ii} \log_2 \rho_{ii},$$

$$R_2 = \Gamma(p) \quad (15)$$

$$p = \frac{1 + \sqrt{[1 - 2(\rho_{33} + \rho_{44})]^2 + 4(|\rho_{14}| + |\rho_{23}|)^2}}{2}$$

where  $\lambda_k$  being the four eigenvalues of the density matrix  $\rho$  and  $\Gamma(x) = -x \log_2 x - (1-x) \log_2 (1-x)$ . As the density matrix of our system  $\rho$  in Equation (9) is X states. In Fig.3, we explore how

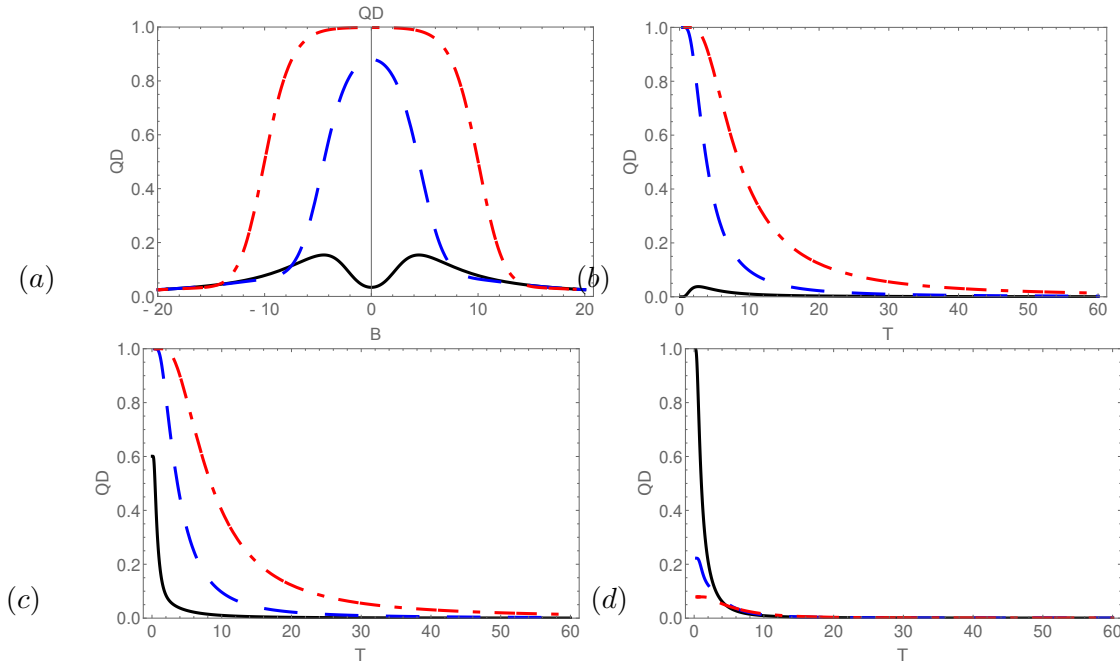


**Figure 3:** (a) The evolution of Quantum Discord (QD) in terms of B. The solid, dashed and dot-dashed curves are evaluated for  $D = 0, 5, 10$ , respectively, with  $T = 2$ . The QD as a function of temperature T. The solid, dashed and dot-dashed curves are evaluated for  $D = 0, 5, 10$ , respectively where in (b)  $B = 0$ , (c)  $B = 2$  and in (d) the solid, dashed and dot-dashed curves are evaluated for  $B = 1, 5, 10$ , respectively, with  $D = 2$ . ( $\gamma = 2, J = 1$ )

a quantum dot (QD) behaves in a two-qubit spin chain and how factors such as DM interaction, magnetic field strength, and temperature affect it. In Fig.3(a), we depict the QD function as a symmetrical curve B at a temperature of  $T = 2$  while keeping the DM interaction constant—the curve peaks when  $B = 0$ , indicating that the parameter is deteriorating. Additionally, the QD function is significantly influenced by the different values of  $D_z$  concerning B. As observed, the QD function increases as  $D_z$  increases, reaching its maximum at  $D_z = 10$ . However, as  $D_z$

increases, the QD preservation width also increases. Fig.3(b) delves into the dynamics of QD under DM interaction, characterized by temperature. Increasing  $D_z$  strength can reduce the effect of temperature, as demonstrated by the fact that QD is more efficient at  $D_z = 10$  and less efficient at  $D_z = 0$  when the temperature is applied. In Fig.3(c), we examine the impact of a magnetic field on the QD function, which is characterized by temperature. When  $D_z = 10$ , the QD persists for an extended period, while it lasts for a shorter time when  $D_z = 0$ .

In Figure 3(d), we can see how a magnetic field affects the dynamical map of a quantum discord (QD). The more intense the magnetic field, the more it damages the QD's function, indicating that it is deteriorating. The strength of the field also determines the preservation interval and initial values of the QD in two qubits. At a magnetic field value of 10, the minimum initial QD value can be observed. The dynamical map of the two-qubit QD is monotonic, with no observed relative revivals, unlike the results for entanglement and QD, which display clear revival characteristics Zidan (2014). Consequently, under the current system-cavity couplings, there is a permanent loss of quantum information. In Figure 4, we explore the combined impact

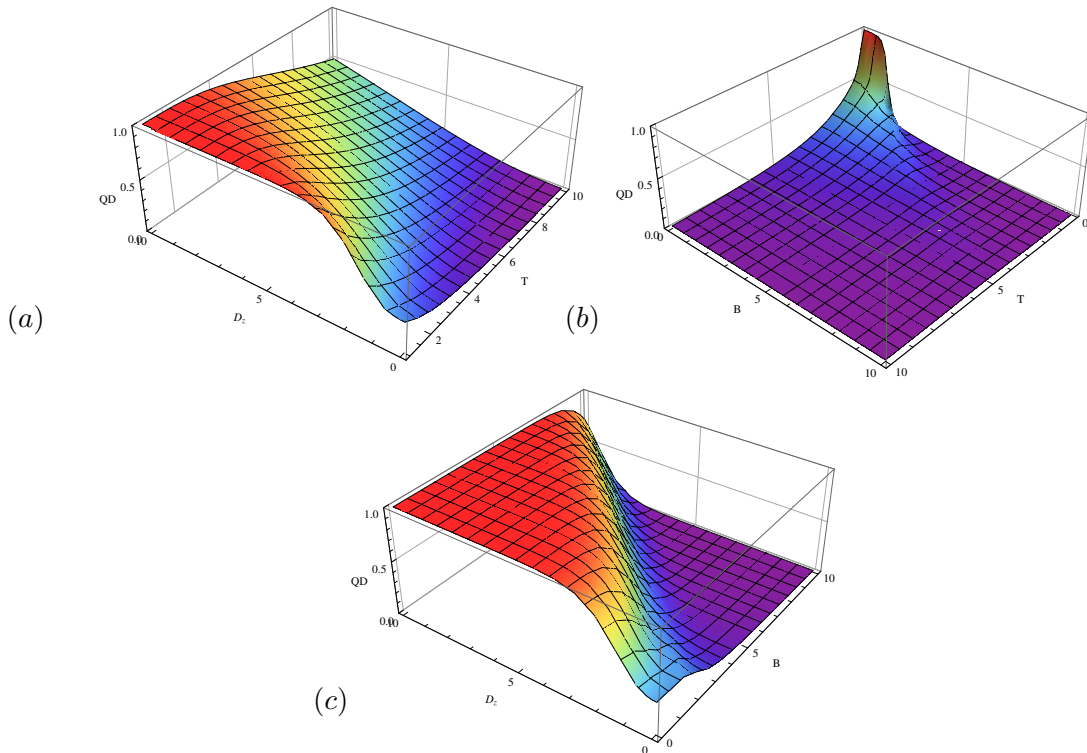


**Figure 4:** The evolution of Quantum Discord (QD) against the different parameters. In (a) be plotted between  $T$ ,  $D_z$  at  $B = 1$ , (b) be plotted between  $T$ ,  $B$  at  $D_z = 1$ , (c) be plotted between  $B$ ,  $D_z$  at  $T = 1$ . ( $\gamma = 2, J = 1$ )

of the DM interaction, magnetic field strength, and temperature on the dynamical map of a two-qubit QD. The QD is highly sensitive to changes in relative parameter values, which dictate its initial values and preservation intervals. Figure 4(a) displays the joint effects of  $T$  and  $D_z$ , revealing that the QD function improves as  $D_z$  increases but decreases with increasing  $T$  values. When we investigate the combined effects of  $B$  and  $T$  in Figure 4(b), we find that the QD function is inversely affected by both parameters and as the values of  $B$  and  $T$  increase, the QD function decays to 0 more quickly. Finally, in Figure 4(c), we analyze the effects of  $B$  and  $D_z$  and find that they have opposite effects on QD preservation. As  $D_z$  increases, QD tends to conserve, whereas the findings for  $B$  are contradictory.

## 5 Conclusions

This study examined the dynamic mappings of QFI and QD in a two-qubit spin chain with a Dzyaloshinskii-Moriya interaction linked to a non-local cavity. We hypothesize that the non-local cavity is controlled by temperature and magnetic field intensity. Our findings reveal that the QFI and QD functionalities are vulnerable and easily lost when exposed to current fields, with the factors involved being the only determinants of decay behavior and quantity. Instead of studying the essential Dzyaloshinskii-Moriya interaction, we focused on the influence of the z-component interaction parameter ( $D_z$ ) of the same interaction. The  $D_z$  parameter is critical for preserving QFI and QD functions.

Although temperature and magnetic strength were predicted to weaken QFI and QD, increasing  $D_z$  can counteract these adverse effects. Thus, we hope our research can assist in the practical design of quantum cavities and interactions of a similar kind to preserve quantum phenomena better.

## References

- Abdel-Hameed, H., Zidan, N., & Metwally, N. (2018). Quantum Fisher information of two superconducting charge qubits under dephasing noisy channel. *International Journal of Modern Physics B*, 32(22), 1850245.
- Abdel-Khalek, S., Abd-Elmougod, G.A. & El-Sayed, M.A. (2017). Some features of quantum fisher information and entanglement of two atoms based on atomic state estimation. *Applied Mathematics & Information Sciences*, 11(3), 677-681.
- Akyuz, C., Aydiner, E., & Mustecaploglu, O.E. (2008). Thermal entanglement of a two-qutrit Ising system with Dzialoshinski–Moriya interaction. *Optics Communications*, 281(20), 5271-5277.
- Alenezi, M., Zidan, N., Alhashash, A., & Rahman, A.Ur. (2023). Quantum Fisher information for two-qubit XY spin-chain: individual characterization of different parameters. *Optical and Quantum Electronics*, 55, 426.
- Alenezi, M., Zidan, N., Alhashash, A., & Rahman, A.Ur.(2022). Quantum Fisher Information Dynamics in the Presence of Intrinsic Decoherence. *International Journal of Theoretical Physics*, 61, 1.
- Apellaniz, I., lucke, B., Peise, J., Klempt, C., & Toth, G. (2015). Detecting metrologically useful entanglement in the vicinity of Dicke states. *New Journal of Physics*, 17, 083027.
- Bakry, H., Mohamed, A.S.A., & Zidan, N. (2018). Properties of Two Two-level Atoms Interacting with Intensity-Dependent Coupling. *International Journal of Theoretical Physics*, 57(2), 539-548.
- Banerjee, S., Alok, A.K., & Omker, S. (2016). Quantum Fisher and skew information for Unruh accelerated Dirac qubit. *The European Physical Journal C*, 76, 437.
- Boixo, S., Flammia, S.T., Caves, C.M., & Geremia, J.M. (2007). Generalized Limits for Single-Parameter Quantum Estimation. *Physical Review Letters*, 98, 090401.
- Boixo, S., Monras, A. (2008). Operational Interpretation for Global Multipartite Entanglement. *Physical Review Letters*, 100, 100503.
- Braunstein, S.L., Caves, C.M., Milburn, G.J. (1996). Generalized Uncertainty Relations: Theory, Examples, and Lorentz Invariance, *Annals of Physics*, 247, 135-173.

- Chentsov, N.N. (1982). *Statistical Decision Rules and Optimal Inference*. Nauka Moscow. English translation, AMS, Rhode Island(in Russian).
- Cremér, H. (1946). *Mathematical Methods of Statistics*. Princeton University.
- Dzyaloshinskii, I.A. (1958). A thermodynamic theory of “weak” ferromagnetism of antiferromagnetics. *Journal of Physics and Chemistry of Solids*, 4, 241-255.
- El-Sayed, A., Arafa, A., Hanafy, I., & Hagag, A. (2023). An Approximate Study of Fisher’s Equation by Using a Semi-Analytical Iterative Method, *Progress in Fractional Differentiation and Applications*, 9(3), 397-407.
- El-Sanousy, E., Tolan, M., Abouelsaad, I.A., Abd-Elhamed, A., & Abdel-Hameed, H.F. (2021). New Quantum Algorithms using Multi-Qubit Interaction. *Information Sciences Letters*, 10(3), 445-450.
- Fakharany, M., El-Abed, A., Elzawy, M., & Mosa, S. (2022). On the Geometry of E quiform Normal Curves in the Galilean Space  $G^4$ , *Information Sciences Letters*, 11(5), 1711-1715.
- Fisher, R.A. (1925). Theory of Statistical Estimation. *Proceedings of the Cambridge Philosophical Society*, 22(5), 700-725.
- Gaaz, T.S., Dakhil, R.M., Jamil, D.M., Al-Amiery, A.A., Kadhum, A.A., & Takriff, M. (2020). Evaluation of Green Corrosion Inhibition by Extracts of Citrus aurantium Leaves Against Carbon Steel in 1 M HCl Medium Complemented with Quantum Chemical Assessment, *International Journal of Thin Films Science and Technology*, 9(3), 171-179.
- Ganaie, R.A., Rajagopalan, V., & Aldulaimi, V. (2021). The Weighted Power Shanker Distribution with Characterizations and Applications of Real Life Time Data. *Journal of Statistics Applications & Probability*, 10(1), 245-265.
- Gibilisco, P., Imparato, D. & Isola, T. (2007). Uncertainty principle and quantum Fisher information II. *Journal of Mathematical Physics*, 48(7), 072109
- He, Q., Xu, J.B. (2011). Tunable entanglement sudden death and three-partite entanglement in Tavis–Cummings model with an added nonlinear kerr-like medium. *Optics Communications*, 284(6), 1714-1718.
- Ibrahim, M. (2020). Optimal control of a fishery utilizing compensation and critical depensation models. *Applied Mathematics & Information Sciences*, 14(3), 467-479.
- Invernizzi C., Korbman M., Venuti L.C. & Paris M.G.A. (2008). Optimal quantum estimation in spin systems at criticality, *Physical Review A*, 78, 042106
- Jing, X.X., Liu, J., Zhong, W., & Wang, X.G. (2014). Quantum Fisher Information of Entangled Coherent States in a Lossy Mach–Zehnder Interferometer. *Communications in Theoretical Physics*, 61, 115-120.
- Korashy, S.T., Al-Bayatti, H., & El-Shahat, T.M. (2021). Statistical Properties of the Nonlinear Time-dependent Interaction between a Three-level Atom and Optical Fields, *Journal of Statistics Applications & Probability*, 10(3), 779-793.
- Lazopoulos, K.A., Lazopoulos, A.K. (2016). Fractional Differential Geometry of Curves & Surfaces, *Progress in Fractional Differentiation and Applications*, 2(3), 169-186
- Liu, T.K., Tao, Y., Shan, C.J., & Liu, J.B. (2017). Quantum Entanglement and Correlation of Two Qubit Atoms Interacting with the Coherent State Optical Field. *International Journal of Theoretical Physics*, 56, 3232-3243.

- Liao, Q., Fang, G., Ahmed, A., & Liu, S. (2011). Sudden birth of entanglement between two atoms successively passing a thermal cavity. *Optics Communications*, 284(1), 301-305.
- Luo, S. (2004). Wigner-Yanase skew information vs. quantum Fisher information. *Proceedings of the American Mathematical Society*, 132, 885-890.
- Luo, S. (2000). Quantum Fisher Information and Uncertainty Relations. *Letters in Mathematical Physics*, 53, 243-251.
- Ma, J., Huang, Y.X., Wang, X., & Sun, C.P. (2011). Quantum Fisher information of the Greenberger-Horne-Zeilinger state in decoherence channels. *Physical Review A*, 84, 022302.
- Ma, J., Wang, X. (2009). Fisher information and spin squeezing in the Lipkin-Meshkov-Glick model. *Physical Review A*, 80, 012318.
- Metwally, N. (2018). Fisher information of accelerated two-qubit systems. *International Journal of Modern Physics B*, 32(5), 1850050.
- Metwally N. (2017). Estimation of teleported and gained parameters in a non-inertial frame. *Laser Physics Letters*, 14, 045202.
- Moriya, T. (1960). Theory of Magnetism of  $NiF_2$ . *Physical Review*, 117(3), 635-647.
- Oleiwi, M.O., Akoosh, D.J., & Ajeel, S.K. (2023). Evaluation of Temperature Effects for Quantum Cascade Laser Dynamics (QCLs). *International Journal of Thin Films Science and Technology*, 12(2), 141-146.
- Ozaydin, F., Altintas, A.A. (2020). Parameter estimation with Dzyaloshinskii-Moriya interaction under external magnetic fields. *Optical and Quantum Electronics*, 52, 70.
- Redwan, A., Abdel-Aty, A., Zidan, A., & El-Shahat, T. (2018). Dynamics of Classical and Quantum Information on Spin-chains with Multiple Interactions. *Information Sciences Letters*, 7(2), 29-33.
- Redwan A., El-Shahat T. (2017). Study the Entanglement Dynamics of an Anisotropic Two-Qubit Heisenberg XYZ System in a Magnetic Field *Journal of Quantum Information Science*, 7(4), 160-171.
- Reyad, O. (2018). Text Message Encoding Based on Elliptic Curve Cryptography and a Mapping Methodology. *Information Sciences Letters*, 7(1), 7-11.
- Rosa, M., Bruzón, M.S., & Gandarias M.L. (2015). Lie Symmetry Analysis and Conservation Laws for a Fisher Equation with Variable Coefficients. *Applied Mathematics & Information Sciences*, 9(6), 2783-2792.
- Salvatori, G., Mandarino, A., & Paris, M.G.A. (2014). Quantum metrology in Lipkin-Meshkov-Glick critical systems. *Physical Review A*, 90, 022111.
- Song, X., Wua, T., & Ye, L. (2014). Quantum correlations and quantum phase transition in the Ising model with Dzyaloshinskii-Moriya interaction. *Physica A*, 394, 386-393.
- Sun, Z., Ma, J., Lu, X.M., & Wang, X. (2010). Fisher information in a quantum-critical environment. *Physical Review A*, 82, 022306.
- Sweilam, N.H., Abou Hasan, M.M. (2016). Numerical Studies for the Fractional Schrodinger Equation with the Quantum Riesz-Feller Derivative. *Progress in Fractional Differentiation and Applications*, 2(4), 231-245.

- Tawhid, M.A., Gu, W.Z. (2016). Global Error for Generalized Complementarity Problems based on Generalized Fisher-Burmeister Function. *Applied Mathematics & Information Sciences*, 10(1), 135-142.
- Xu, X.H., Chen, M.W.(2018). The Rod Eutectic Growth under Rapid Solidification Conditions. *International Journal of Thin Films Science and Technology*, 7(1), 35-42.
- Yan, X.Q., Zhang, B.Y. (2014). Collapse–revival of quantum discord and entanglement. *Annals of Physics*, 349, 350-356.
- Yazdani, A.B., Kiasari, M.M., & Jafari, H. (2021). A Novel Approach for Solving Time Fractional Nonlinear Fisher’s Equation by Using Chebyshev Spectral Collocation Method. *Progress in Fractional Differentiation and Applications*, 7(2), 97-102
- Zhang, G.F. (2007). Thermal entanglement and teleportation in a two-qubit Heisenberg chain with Dzyaloshinski-Moriya anisotropic antisymmetric interaction. *Physical Review A* 75, 034304.
- Zhu, Y.Y., Zhang, Y. (2012). Quantum discord in the three-spin XXZ chain with Dzyaloshinskii-Moriya interaction. *Science China Physics, Mechanics and Astronomy*, 55, 2081.
- Zidan N., Abel-Hameed H., & Metwally N. (2019). Quantum Fisher information of atomic system interacting with a single cavity mode in the presence of Kerr medium. *Scientific Reports*, 9, 2699.
- Zidan, N. (2014). Quantum Discord of a Two-Qubit Anisotropy XXZ Heisenberg Chain with Dzyaloshinskii-Moriya Interaction. *Journal of Quantum Information Science*, 4(2), 104-110.
- Zidan, N. (2014). Entanglement and Quantum Discord of Two Moving Atoms. *Applied Mathematics*, 5, 2485-2492.